Sensors and Materials, Vol. 34, No. 11 (2022) 4127–4136
MYU Tokyo

S & M 3101

Effect of Annealing Temperatures on Optical and Electrical Properties of TiO_2/Mo Multilayer Films for Photosensor Applications

Chi-Fan Liu,[1] Shih-Chen Shi,[2] Tao-Hsing Chen,[1*] and Guan-Lin Guo[1]

[1]Department of Mechanical Engineering, National Kaohsiung University of Science and Technology
No. 415, Jiangong Rd., Sanmin Dist., Kaohsiung City 807618, Taiwan
[2]Department of Mechanical Engineering, National Cheng Kung University (NCKU),
No. 1 University Road, Tainan 70101, Taiwan

(Received June 2, 2022; accepted October 26, 2022)

Keywords: TiO_2/Mo, multilayer thin film, optical property, electrical property, sensor

In this study, titanium dioxide (TiO_2) and molybdenum (Mo) with a purity of 99.99% were deposited on a glass substrate under various parameters through RF magnetron sputtering to form TiO_2/Mo bilayer and TiO_2/Mo/TiO_2 multilayer transparent conductive thin films. In addition, the films were annealed in vacuum at various temperatures to adjust their internal crystallization through thermal energy such that they exhibited replacement characteristics and fewer internal defects. After the bilayer films with a Mo-doped metal layer and the TiO_2/Mo/TiO_2 multilayer films were annealed, the thickness, electrical properties, optical properties, surface structure, and figure of merit (FOM) of the thin films were examined. The results indicated that the TiO_2/Mo bilayer films had a low resistivity of 1.97×10^{-1} Ω-cm before annealing and an average transmittance rate of 66.59%; the unannealed TiO_2/Mo/TiO_2 multilayer films had a resistivity of 7.21×10^{-3} Ω-cm and an average transmittance rate of 69.34%. The optical transmittance of both structures tended to increase with their annealing temperature, and an optimal light transmittance rate of 77% was achieved. For the FOM, the optimal values of the bilayer and multilayer structures were 5.96×10^{-7} and 4.46×10^{-5} Ω^{-1}, respectively. The results indicate that TiO_2/Mo/TiO_2 thin films are suitable for photosensor applications.

1. Introduction

Transparent conductive oxide (TCO) thin films exhibit excellent conductivity and high optical transmittance in the visible and near-infrared (IR) light spectra. Because of these characteristics, TCO thin films are widely applied in various optoelectronic components, including solar cells, thin film transistors, organic LEDs, and flat panel displays.[(1)] In general, metal films are opaque in the visible light spectrum. However, metal films with a thickness of <100 Å can be penetrated by visible light and exhibit strong reflectivity in

*Corresponding author: e-mail: thchen@nkust.edu.tw
https://doi.org/10.18494/SAM4133

ISSN 0914-4935
https://myukk.org/

the IR light spectrum. To produce a semiconductor, materials with an energy gap of >3 eV (e.g., zinc oxide [ZnO], indium (III) oxide [In_2O_3], titanium dioxide [TiO_2], tin oxide [SnO_2], and cadmium oxide [CdO]) must be used.[2]

Generally, semiconductors made of pure elements have poor conductivity; thus, they are not widely used except in sensors of special properties. To improve the electrical properties of a semiconductor, the concentration and characteristics of conductive carriers are adjusted by adding special impurities; this process is called doping. To avoid a lattice mismatch during the doping of various elements, dopants of similar lattice constants or atomic radii are usually used. If the doping element is larger than the original element, the lattice becomes distorted and electron migration is hindered, leading to the deterioration of electrical properties. Therefore, doping substitution can generate more free electrons or electron holes, and the common methods involve the use of Sn-doped ZnO,[3,4] Al-doped ZnO,[5–8] F-doped SnO_2,[9–11] and Ga-doped ZnO.[12–15]

To improve optical transmittance and electrical properties, numerous studies have proposed the use of oxide and metal films as double- or triple-layer structures to form trilayer films with an oxide/metal/oxide or metal oxide/metal/metal oxide arrangement (i.e., sandwich structure films). This type of thin film structure can suppress the reflection of the intermediate metal layer in the visible region and achieve increased transmittance.[16]

In the present study, thin films with TiO_2 (deposited through RF magnetron sputtering) were used to form thin films with bilayer and sandwich structures. After the optimal single-layer parameters were identified, the use of Mo as the intermediate metal layer was tested. Finally, the multilayer structures of the fabricated bilayer Mo/TiO_2 and trilayer TiO_2/Mo/TiO_2 (TMT) films were annealed, and the sandwich multilayer structure with the optimal qualities was identified on the basis of its electrical and optical properties. This structure can be used in a photosensor to obtain excellent optical and electrical properties.

2. Experimental Materials and Methods

In this study, multilayer thin films with different structures were deposited by varying parameters such as sputtering power, sputtering time, and annealing temperature. First, the optimal process parameters for a single-layer TiO_2 film were identified through testing. Theoretically, a thicker film has poorer optical properties but more favorable electrical properties. After tests were conducted, the following parameters were selected for the TiO_2 single layer: a power rate of 100 W, a fixed bias of 6 mTorr, a gas flow rate of 15 sccm, and a sputtering time of 90 min. For the Mo metal layer, the following parameters were selected: a power rate of 20 W, a fixed bias of 10 mTorr, a gas flow rate of 15 sccm, and a sputtering time of 1 min. The first and third TiO_2 layers shared the same parameters, and they were used to form a sandwich structure in which the metal layer was deposited between these two oxide layers; consequently, the metal layer can be easily attached and uniformly deposited during deposition. In the present experiment, a surface profiler (α-step, KLA-Tencor) was used to measure the film thickness on the basis of the height difference. For optical properties, the average transmittance in the visible region decreased from an average of 95% to approximately 70%; during annealing

process, the metal layer was able to diffuse to the top and bottom oxide layers to reduce the poor resistivity caused by the spillage of the metal layer. The annealing temperature was set to 200–500 °C. The thicknesses of the bilayer and sandwich thin films were measured. A Hall measurement system and a spectrophotometer were used to measure the electrical conductivity and penetration of the bilayer and sandwich films, respectively, and X-ray diffraction (XRD) was performed to verify the film structure. Finally, surface topography and roughness analyses were respectively performed using scanning electron microscopy (SEM, Philips XL-40 FEG) and atomic force microscopy (AFM, Digital Instruments D5000). The thickness, conductivity, visible light transmittance, surface morphology, structural properties, and temperature of the annealed and unannealed films were measured by XRD, SEM, spectrophotometry, and Hall measurement to collect data for further analysis.

3. Results and Discussion

3.1 XRD properties of thin films after annealing

In this study, the α-step was used to measure the thickness of the bilayer films with Mo and the multilayer films with the sandwich structure. It was found that the thickness of multilayer thin films did not change after annealing.

Figures 1 and 2 respectively present the structural properties of the bilayer and multilayer films doped with Mo as their intermediate layer. Before annealing, the bilayer films were entirely amorphous and no crystalline phase was identified. Because Mo ions were uniformly distributed in the TiO_2 lattice, no obvious MoO_3 peak was observed. A previous study revealed that Mo ions in a TiO_2 lattice can inhibit grain growth;[17] thus, the lattice remains amorphous and lacks a crystalline phase when it is annealed at 500 °C.

When the TMT films were annealed at 400 °C, a crystalline phase started to appear, and (101), (200), (105), and (211) peaks were detected at 25.2, 48.2, 54.2, and 55.3°, respectively; these

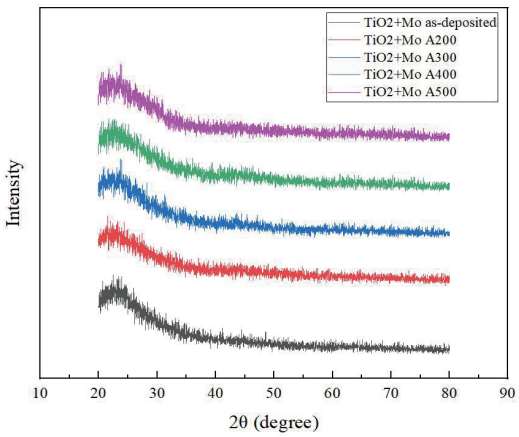

Fig. 1. (Color online) XRD spectra of TiO_2/Mo films under various annealing temperatures.

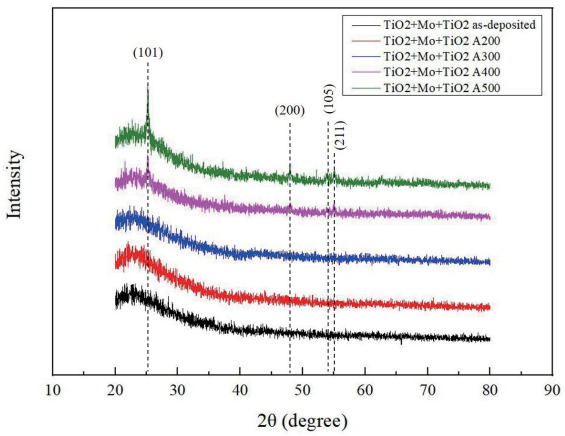

Fig. 2. (Color online) XRD spectra of TMT films under various annealing temperatures.

were all peaks of TiO_2. These results indicated that (101) of the TMT films was the main growth direction and that the growth occurred mainly along the C-axis perpendicular to the substrate. Because the main peak of MoO_3 is similar to that of anatase (101), they are difficult to distinguish from each other. When the annealing temperature was increased to 500 °C, the crystallization peak was considerably enhanced (i.e., crystallization properties were improved). Studies have revealed that increasing the energy of atomic activity produces interstitial atoms, dislocations, and voids that would otherwise be immobile to decrease in number and accumulate on the grain boundary surface, resulting in the disappearance of a large number of pre-equilibrium defects and the release of stress. Consequently, the lattice becomes more ordered and its winding peak is shifted to the right.[18,19]

3.2 Comparison of electrical properties of thin films after annealing

The electrical properties of the TiO_2/Mo films are presented in Table 1. The results indicated that the TiO_2/Mo films had a low resistivity (1.97×10^{-1} Ω-cm) before annealing. At the annealing temperatures of 200 and 300 °C, the TiO_2/Mo films exhibited favorable electrical properties because the doped Mo could diffuse into the TiO_2 layer (where mixing and replacement could occur) after annealing. When the annealing temperature was increased, the resistivity of the films also increased, which led to poor electrical properties; because the temperature required for nanoscale TiO_2 to undergo an anatase-to-rutile transformation is approximately 500–600 °C and anatase exhibits greater fluidity than rutile, anatase is more suitable for use as TCO. When the annealing temperature approached the conversion temperature, grain arrangement and growth were inhibited, which reduced the resistivity of the TiO_2/Mo films.

Table 2 presents the electrical properties of the TMT multilayer films under various annealing temperatures. The TMT multilayer films had a low electrical resistivity of 7.21×10^{-3} Ω-cm before annealing. When the annealing temperature was increased, the resistivity of the films gradually increased; when the annealing temperature reached 500 °C, the resistivity of the films increased to 4.68×10^{-2} Ω-cm. This phenomenon is similar to that observed with the TiO_2/Mo bilayer films, and both phenomena occurred for similar reasons.

Table 1
Electrical properties of TiO_2/Mo films under various annealing temperatures.

TiO_2/Mo: TiO_2 100 W 60 min/Mo 20 W 1 min			
Annealing temperature (°C)	Resistivity (Ω-cm)	Mobility (cm^2/Vs)	Carrier concentration (cm^{-3})
as-deposited	1.97×10^{-1}	7.55	4.82×10^{19}
200	2.27×10^{-1}	6.73	2.48×10^{19}
300	4.95×10^{-1}	6.06	1.56×10^{19}
400	1.03×10^{1}	2.21	4.96×10^{12}
500	2.09×10^{1}	1.83	7.10×10^{12}

Table 2
Electrical properties of TMT films under various annealing temperatures.

TMT: TiO_2 100 W 90 min/Mo 20 W 1 min			
Annealing temperature (°C)	Resistivity (Ω-cm)	Mobility (cm^2/Vs)	Carrier concentration (cm^{-3})
as-deposited	7.21×10^{-3}	21.02	8.44×10^{20}
200	9.17×10^{-3}	20.3	5.52×10^{20}
300	1.52×10^{-2}	16.93	5.09×10^{20}
400	4.32×10^{-2}	15.6	6.60×10^{19}
500	4.68×10^{-2}	15.2	1.24×10^{19}

3.3 Comparison of optical properties of thin films after annealing

Figures 3 and 4 respectively present the optical transmittance properties of the bilayer and multilayer films after annealing at different temperatures. The results indicated that the overall average transmittance was approximately 65–68% for the bilayer films with a Mo metal layer. When the annealing temperature was increased, the overall transmittance remained mostly unchanged. Because of the high refractive index of TiO_2, the main loss was probably caused by reflection.

The energy gap is calculated by applying the optical energy gap formula,[20]

$$(\alpha h\upsilon)^2 = A(h\upsilon - Eg), \tag{1}$$

where A is a constant and α and $h\upsilon$ represent the absorption coefficient and incident radiation energy, respectively. The energy gap of the double-layer films with a Mo layer reached 3.49 eV before annealing and peaked at 3.54 eV when the films were annealed at 500 °C. The relationship between the energy gap and the photon energy for different annealing temperatures is presented in Figs. 5 and 6 for the bilayer and TMT films, respectively. The average transmittance rate of the TMT films increased with the annealing temperature, and the highest transmittance rate of 77.40% was achieved at 500 °C. This phenomenon occurred primarily because the energy of the intermediate metal layer increased with the annealing temperature, allowing the layer to be doped and replaced with upper and lower oxide atoms after gaining energy, which reduced the reflection of visible light by the metal. When the annealing temperature was increased, TiO_2 gradually transformed into its rutile phase, which has a slightly higher transmittance rate than the anatase phase, resulting in an increase in transmittance rate. The TMT films had an energy gap of 3.37 eV before annealing and a maximum energy gap of 3.45 eV after annealing at 500 °C.

3.4 Surface morphology analysis of annealed thin films

The surface morphology of the bilayer thin films was mainly analyzed by AFM. The samples with a Mo-doped metal layer and the samples treated under various annealing temperatures were analyzed and represented using 3D diagrams, and their average roughness (*Ra*) was

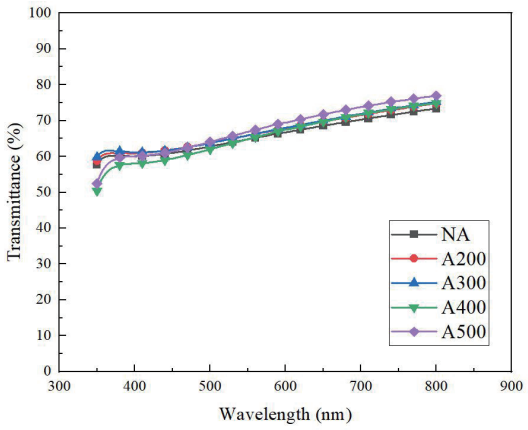

Fig. 3. (Color online) Transmittance of TiO_2/Mo films under various annealing temperatures.

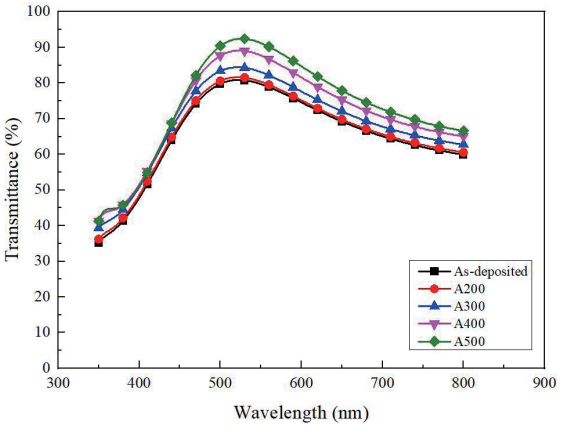

Fig. 4. (Color online) Transmittance of TMT films under various annealing temperatures.

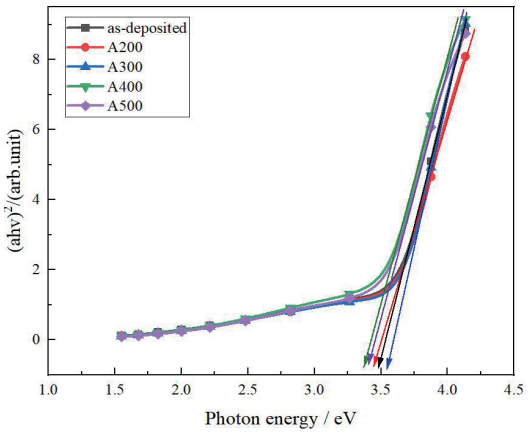

Fig. 5. (Color online) Energy gap of TiO_2/Mo under various annealing temperatures.

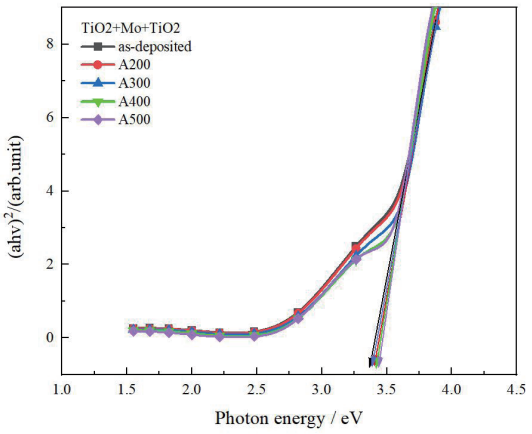

Fig. 6. (Color online) Energy gap of TMT films under various annealing temperatures.

measured. The surface morphology and roughness results for the bilayer films are respectively presented in Table 3 and Fig. 7, which reveal that under various temperatures, the *Ra* values of all the thin films were <1 nm. Furthermore, as the annealing temperature increased, *Ra* decreased. This means that the surface of the bilayer films became denser after annealing.

The overall Ra value of the TMT multilayer films was also <1 nm (Table 3), indicating that their surface was smooth. Additionally, when the annealing temperature was increased, their surface roughness decreased, indicating that annealing effectively reduced the surface roughness of the films (Fig. 8). The roughness of the TMT films decreased because of the rearrangement of their TiO_2 crystals.

Table 3
Roughnesses of bilayer and multilayer films under various annealing temperatures.

	Ra (nm)	
Annealing temperature (°C)	TiO_2/Mo	TMT
as-deposited	0.010.1	0.00973
200	0.00984	0.00901
300	0.00895	0.00890
400	0.0065	0.00887
500	0.00648	0.00862

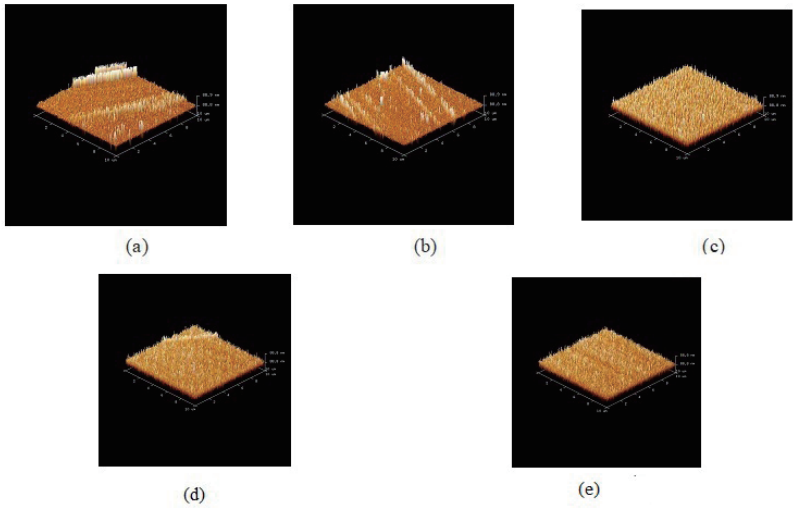

Fig. 7. (Color online) AFM images of TiO_2/Mo films under various annealing temperatures: (a) as-deposited, (b) 200, (c) 300, (d) 400, and (e) 500 °C.

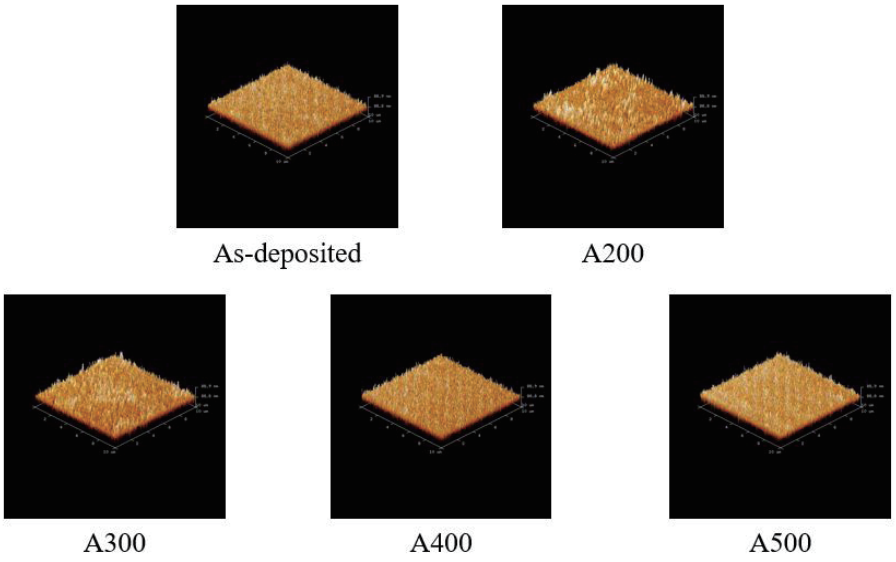

Fig. 8. (Color online) AFM images of TMT films under various annealing temperatures.

Table 4
FOM values of bilayer and multilayer films under various annealing temperatures.

	FOM, $Ø_{TC}$ (Ω^{-1})	
Annealing temperature (°C)	TiO_2/Mo	TMT
as-deposited	5.96×10^{-7}	4.46×10^{-5}
200	5.82×10^{-7}	3.87×10^{-5}
300	2.73×10^{-7}	3.28×10^{-5}
400	1.13×10^{-8}	1.73×10^{-5}
500	1.03×10^{-8}	2.13×10^{-6}

3.5 Figure of merit

For the transparent conductive films, figure of merit (FOM) was used to determine their material quality; resistivity and transmittance were used to calculate the FOM of each bilayer film under various annealing temperatures. According to the formula for calculating FOM, FOM is proportional to the 10th power of the transmittance; therefore, transmittance has a considerable effect on the FOM of a film. A more favorable FOM is achieved with lower resistivity and higher transmittance. The formula for calculating FOM is[21]

$$Ø_{TC} = \frac{T_{av}^{10}}{R_{sh}}, \tag{2}$$

where T_{av} is the average transmittance and R_{Sh} is the sheet resistance. Table 4 reveals that the bilayer and multilayer films exhibited optimal FOM values when they were unannealed (TiO_2/Mo bilayer thin films, 5.96×10^{-7} Ω^{-1}; TMT thin films, 4.46×10^{-5} Ω^{-1}), indicating that annealing had a limited effect on the FOM of these two types of films. The figures reveal that the thin films had low resistivity before annealing. When the annealing temperature increased, the transmittance and resistivity of the films increased, but their FOM decreased after annealing.

4. Conclusions

Our experimental results revealed that the overall thickness of Mo-doped TiO_2 bilayer and multilayer films did not vary significantly under various annealing temperatures. The XRD results revealed that the TMT films were amorphous before annealing and started to form crystalline phases (all of which were peaks for In_2O_3) when they were annealed at 200 °C. This finding suggests that Mo ions were replaced and incorporated into the lattice of In_2O_3, with (400) being the main growth direction. Regarding their electrical properties, the TMT films had a low resistivity of 7.21×10^{-3} Ω-cm before annealing. Regarding their optical transmittance, the TiO_2/Mo bilayer and TMT multilayer films achieved their peak average transmittances of 70.1 and 77.4%, respectively, at 500 °C; they also achieved their highest energy gap values of 3.49 and 3.54 eV, respectively, at 500 °C. The surface roughness data indicated that both the bilayer and multilayer films were smooth. Additionally, when the annealing temperature increased, the

surface roughness of the films decreased, indicating that the annealing effectively reduced the surface roughness of the films. Finally, the two film structures exhibited their optimal FOM values before annealing (TiO_2/Mo bilayer thin films, 5.96×10^{-7} Ω^{-1}; TMT thin films, 4.46×10^{-5} Ω^{-1}). Owing to the excellent optical and electrical properties of the TMT multilayer thin films, such thin films can be applied in photosensors.

Acknowledgments

This paper was produced through Research Project MOST111-2628-E-992-001-MY2, which is supported by the National Science and Technology Council of Taiwan. The authors would like to express their gratitude to the National Science and Technology Council for its support, which enabled the smooth completion of this research.

References

1 T. Wang, H. P. Ma, J. G. Yang, J. T. Zhu, J. Feng, S. J. Ding, H. L. Lu, and D. W. Zhang: J. Alloy Compd. **744** (2018) 381. https://doi.org/10.1016/j.jallcom.2018.02.115
2 C. F. Liu, T. H. Chen, and Y. S. Huang: Sens. Mater. **32** (2020) 2321. https://doi.org/10.18494/SAM.2020.2867
3 E. Peksu and H. Karaagac: J. Alloy Compd. **764** (2018) 616. https://doi.org/10.1016/j.jallcom.2018.06.101
4 S. Ilican, M. Caglar, and Y. Caglar: Appl. Surf. Sci. **256** (2010) 7204. https://doi.org/10.1016/j.apsusc.2010.05.052
5 T. H. Chen, T. C. Cheng, and Z. R. Hu: Microsyst. Technol. **19** (2013) 1787. https://doi.org/10.1007/s00542-013-1837-5
6 P. Misr, V. Ganeshan, and N. Agrawal: J. Alloy Compd. **725** (2017) 60. https://doi.org/10.1016/j.jallcom.2017.07.121
7 E. Arca, K. Fleischer, and I. Shvets: Thin Solid Films **555** (2014) 9. https://doi.org/10.1016/j.tsf.2013.08.110
8 F. H. Wang and C. L. Chang: Appl. Surf. Sci. **370** (2016) 83. https://doi.org/10.1016/j.apsusc.2016.02.161
9 T. Li, X. Zhang, J. Ni, J. Fang, D. Zhang, J. Sun, C. Wei, S. Xu, G. Wang, and Y. Zhao: Solar Energy **134** (2016) 375. https://doi.org/10.1016/j.solener.2016.04.042
10 C. F. Liu, C. H. Kuo T. H Chen, and Y. S. Huang: Coating **10** (2020) 394. https://doi.org/10.3390/coatings10040394
11 C. Y. Tsay, H. C. Cheng, Y. T. Tung, W. H. Tuan, and C. K. Lin: Thin Solid Films **517** (2008) 1032. https://doi.org/10.1016/j.tsf.2008.06.030
12 T. H. Chen and T. Y. Chen: Nanomaterials **5** (2015) 1831. https://doi.org/10.3390/nano5041831
13 T. Y. Tsai, T. H. Chen, S. L. Tu, Y. H. Su, Y. H. Shen, and C. L. Yang: Opt. Quantum Electron. **48** (2016) 475. https://doi.org/10.1007/s11082-016-0745-1
14 F. H. Wang, C. C. Huang, C. F. Yang, and H. T. Tzeng: Int. J. Photoenergy **2013** (2013) 1. https://doi.org/10.1155/2013/270389
15 S. H. Lee, G. Kim, J. W. Lim, K. S. Lee, and M. G. Kang: Sol. Energy Mater. Sol. Cells **186** (2018) 378. https://doi.org/10.1016/j.solmat.2018.07.010
16 M. Y. Yen, T. H. Chen, P. H. Lai, S. L. Tu, and Y. H. Shen: Sens. Mater. **33** (2021) 3941. https://doi.org/10.18494/SAM.2021.3706
17 T. Zhang, B. Yu, D. Wang, and F. Zhou: J. Power Sources **281** (2015) 411. https://doi.org/10.1016/j.jpowsour.2015.02.017
18 W. T. Yen, Y. C. Lin, P. C. Yao, J. H. Ke, and Y. L. Chen: Thin Solid Films **518** (2010) 3882. https://doi.org/10.1016/j.tsf.2009.10.149
19 P. Erhart, K. Albe, and A. Klein: Phys. Rev. B **73** (2006) 205203. https://doi.org/10.1103/PhysRevB.73.205203
20 T. Minami, H. Nanto, and S. Takata: J. Appl. Phys. **24** (1985) L605. https://doi/org/10.1143/JJAP.24.L605
21 G. Haacke: J Appl. Phys. **47** (1976) 4086. https://doi/org/10.1063/1.323240

About the Authors

Chi-Fan Liu received his M.D. degree from the University of the Incarnate Word, U.S.A., in 2002. Since 2004, he has been an associate professor at Feng Chia University, Taiwan. Since 2019, he has been the head of Yuchi Township, Nantou County, Taiwan. He is currently a Ph.D. graduate student at National Kaohsiung University of Science and Technology, Department of Mechanical Engineering, Kaohsiung, Taiwan. His research interests are in thin films, sport science, bioengineering, and sensors. (I108142101@nkust.edu.tw)

Shih-Chen Shi received his B.S. and M.S. degrees from National Cheng Kung University, Taiwan, in 1999 and 2001, respectively, and his Ph.D. degree from National Chiao Tung University, Taiwan, in 2005. From 2007 to 2012, he was the head of the R&D Department at EVERLIGHT Electronic Co., Ltd., Taiwan. Since 2014, he has been an associate professor at National Cheng Kung University. His research interests are in nanomaterials, tribology, LED applications, and sustainable materials. (scshi@mail.ncku.edu.tw)

Tao-Hsing Chen received his B.S. degree from National Cheng Kung University, Taiwan, in 1999 and his M.S. and Ph.D. degrees from the Department of Mechanical Engineering, National Cheng Kung University, in 2001 and 2008, respectively. From August 2008 to July 2010, he was a postdoctoral researcher at the Center for Micro/Nano Science and Technology, National Cheng Kung University. In August 2010, he became an assistant professor at National Kaohsiung University of Applied Sciences (renamed National Kaohsiung University of Science and Technology), Taiwan. Since 2016, he has been a professor at National Kaohsiung University of Science and Technology. His research interests are in metal materials, TCO thin films, thermal sensors, and photosensors. (thchen@nkust.edu.tw)

Guan-Lin Guo received his B.S. degree from National Kaohsiung University of Science and Technology, Taiwan, where he is currently studying toward his M.S. degree. His research interests are in MEMS, materials engineering, and sensors. (F109142170@nkust.edu.tw)